All-optical chaotic MQW laser repeater for long-haul chaotic communications

Senlin Yan (颜森林)

Department of Physics, Nanjing Xiaozhuang College, Nanjing 210017

Received October 20, 2004

We present an all-optical chaotic multi-quantum-well (MQW) laser repeater system to be used in long-haul chaotic communications. Chaotic synchronization is achieved among transmitter, repeater, and receiver. Chaotic repeater communications with a sinusoidal signal of 0.2-GHz modulation frequency and a digital signal of 0.4-Gb/s bit rate are numerically simulated, respectively. Calculation results illustrate that the signals are well decoded by the chaotic repeaters. Its bandwidth and the characteristics at much high bit rate are also analyzed. Simulation shows that the repeater can improve decoding quality, especially in higher bit rate chaotic communications.

OCIS codes: 140.1540, 140.3460, 120.4640, 060.4510.

Chaos is very sensitive to its initial conditions and can produce many different infinite dense traces in phase space. Its waveform varies disorderedly and complicatedly with a pseudorandom oscillation characteristics and its dynamic behavior can be hardly predicted[1−3]. Therefore, chaos has been applied widely in secure communications. So the chaotic secure communications have been studied intensively during recent years[4−7]. All-optical chaotic laser system shows a larger bandwidth and lower attenuation, its kinetic system is complicated and very sensitive to parameters, so it can be used to encode more information. Furthermore, photon is hardly falsified so that the system is more secure. Hence, the optical chaotic systems are suitable for long-haul secure communications[4−7].

Generally, the amplitude of signal becomes smaller because of the channel losses during its transmission process in long-haul communication system. This leads to demodulation difficulty in receiver. At the same time, the phase of signal also varies, and then it is difficult to restore the original signal. Besides, the influences of transmission channel and other factors can also make the signal produce unpredictable changes. In addition, establishing chaotic communication repeater system is still relative to variable characteristics of chaotic signal itself. Chaos is greatly sensitive to noise and other external perturbation, the receiver hardly synchronizes with the transmitter so that the demodulating signal cannot be realized. To solve the problems, here we propose to use chaotic repeaters in long-haul optical chaotic communication system to reform the transmitted signal and restore the original signal.

In this letter, we present a model of all-optical chaotic multi-quantum-well (MQW) laser repeater. Synchronization is numerically achieved among a transmitter, a repeater, and a receiver. The repeater encoding and its bandwidth are also simulated and analyzed.

Figure 1 shows the scheme of all-optical chaotic repeater. The transmitter, the repeater, and the receiver are made of identical master (M) and slave (S) graded-index separate confinement heterostructure (GRIN-SCH) MQW laser diodes (LDs)[7,8], and feedback paths are contained in the repeater S-LD and the receiver S-LD, respectively. M-LD output lasing field $E_{\mathrm{m}}\exp[-j(\omega_{\mathrm{m}}t+\phi_{\mathrm{m}})]$ is injected into S-LD, and then S-LD output lasing field $E(t)\exp\{-j[\omega_{\mathrm{m}}t+\phi(t)]\}$ goes into chaos. The receiver factor and the feedback coefficient are supposed as f. We also assume that the repeater has the same structure and characteristic as the receiver, and it receives transmitted signal and synchronizes with the received signal. At the same time, it can transmit the regenerated signal to next repeater. According to this configuration, we describe S-LDs output lasing fields by Lang-Kobayshi equations[7,8] as

$$\frac{\mathrm{d}E_{\mathrm{t,r1}}}{\mathrm{d}t}=\frac{1}{2}(G_{\mathrm{t,r1}}-\gamma_{\mathrm{p}})E_{\mathrm{t,r1}}+\frac{k}{\tau_{\mathrm{L}}}E_{\mathrm{m}}\cos(\phi_{\mathrm{m}}-\phi_{\mathrm{t,r1}})+n_{\mathrm{r}}\frac{f}{\tau_{\mathrm{L}}}[E_{\mathrm{t}}\cos(\phi_{\mathrm{t}}-\phi_{\mathrm{r1}})-E_{\mathrm{r1}}],$$

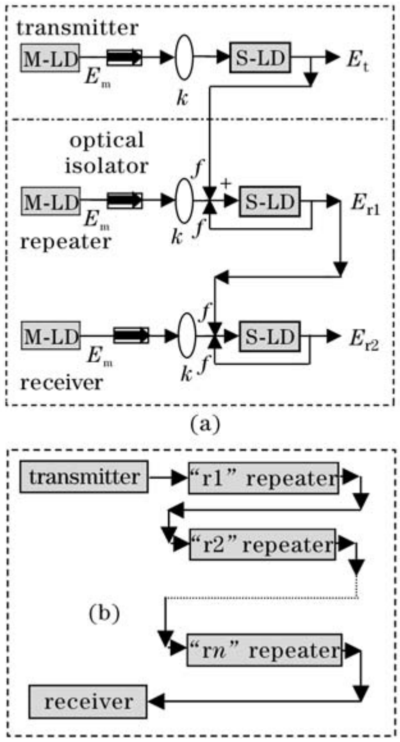

Fig. 1. Schematic of all-optical chaotic repeater. (a) illustrates transmitter, receiver, and repeater, respectively. (b) illustrates a series of repeaters.

$$\frac{\mathrm{d}\phi_{\mathrm{t,r1}}}{\mathrm{d}t} = \frac{1}{2}\beta_{\mathrm{c}}(G_{\mathrm{t,r1}}-\gamma_{\mathrm{p}}) + \frac{k}{\tau_{\mathrm{L}}}\frac{E_{\mathrm{m}}}{E_{\mathrm{t,r1}}}\sin(\phi_{\mathrm{m}}-\phi_{\mathrm{t,r1}}) -\Delta\omega_{\mathrm{m}} + n_{\mathrm{r}}\frac{f}{\tau_{\mathrm{L}}}\frac{E_{\mathrm{t}}}{E_{\mathrm{r1}}}\sin(\phi_{\mathrm{t}}-\phi_{\mathrm{r1}}),$$

$$\frac{\mathrm{d}N_{\mathrm{Bt,r1}}}{\mathrm{d}t} = \eta_{\mathrm{i}}\frac{I}{q} - \gamma_{\mathrm{BQ}}N_{\mathrm{Bt,r1}} + \gamma_{\mathrm{QB}}N_{\mathrm{t,r1}},$$

$$\frac{\mathrm{d}N_{\mathrm{t,r1}}}{\mathrm{d}t} = \gamma_{\mathrm{BQ}}N_{\mathrm{Bt,r1}} - (\gamma_{\mathrm{et,r1}}+\gamma_{\mathrm{QB}})N_{\mathrm{t,r1}} - G_{\mathrm{t,r1}}V_{\mathrm{p}}E_{\mathrm{t,r1}}^2, \quad (1)$$

and

$$\frac{\mathrm{d}E_{\mathrm{r2}}}{\mathrm{d}t} = \frac{1}{2}(G_{\mathrm{r2}}-\gamma_{\mathrm{p}})E_{\mathrm{r1,r2}} + \frac{k}{\tau_{\mathrm{L}}}E_{\mathrm{m}}\cos(\phi_{\mathrm{m}}-\phi_{\mathrm{r2}}) + n_{\mathrm{r}}\frac{f}{\tau_{\mathrm{L}}}[E_{\mathrm{r1}}\cos(\phi_{\mathrm{r1}}-\phi_{\mathrm{r2}}) - E_{\mathrm{r2}}],$$

$$\frac{\mathrm{d}\phi_{\mathrm{r2}}}{\mathrm{d}t} = \frac{1}{2}\beta_{\mathrm{c}}(G_{\mathrm{r2}}-\gamma_{\mathrm{p}}) + \frac{k}{\tau_{\mathrm{L}}}\frac{E_{\mathrm{m}}}{E_{\mathrm{r2}}}\sin(\phi_{\mathrm{m}}-\phi_{\mathrm{r2}}) - \Delta\omega_{\mathrm{m}} + n_{\mathrm{r}}\frac{f}{\tau_{\mathrm{L}}}\frac{E_{\mathrm{r1}}}{E_{\mathrm{r2}}}\sin(\phi_{\mathrm{r1}}-\phi_{\mathrm{r2}}),$$

$$\frac{\mathrm{d}N_{\mathrm{Br2}}}{\mathrm{d}t} = \eta_{\mathrm{i}}\frac{I}{q} - \gamma_{\mathrm{BQ}}N_{\mathrm{Br2}} + \gamma_{\mathrm{QB}}N_{\mathrm{r2}},$$

$$\frac{\mathrm{d}N_{\mathrm{r2}}}{\mathrm{d}t} = \gamma_{\mathrm{BQ}}N_{\mathrm{Br2}} - (\gamma_{\mathrm{er2}}+\gamma_{\mathrm{QB}})N_{\mathrm{r2}} - G_{\mathrm{r2}}V_{\mathrm{p}}E_{\mathrm{r2}}^2, \quad (2)$$

where footnote "t" denotes the transmitter. $n_{\mathrm{r}} = 0$ is for the transmitter and $n_{\mathrm{r}} = 1$ for others. Footnote "r1" denotes the repeater, and footnote "r2" denotes the receiver. For multiple-repeater systems, we transform footnote "r1" in Eq. (2) into footnote "r2", "r2" into "r3", so footnote "r2" represents the second repeater "2", footnote "r3" represents receiver, and the like. Similarly, let "r$(n+1)$" (where $n = 1, 2, 3, \cdots$) represent the receiver, we can establish a series of n-repeater.

E, ϕ, N_{B}, and N in Eqs. (1) and (2) indicate slowly varying field amplitude, phase, carrier numbers in the barrier region and in the active region, respectively. The nonlinear mode gain is given by $G = (\Gamma g_0 v_{\mathrm{g}})/(1 + E^2/E_{\mathrm{s}}^2)\lg\{(N+N_{\mathrm{s}})/(N_{\mathrm{t0}}+N_{\mathrm{s}})\}$, where v_{g} is group velocity of photon in laser cavity, g_0 is the gain constant, E and E_{s} are normalized in such a way that $E = \sqrt{P/V_{\mathrm{p}}}$ and $E_{\mathrm{s}} = \sqrt{P_{\mathrm{s}}/V_{\mathrm{p}}}$ are the optical field amplitudes at saturation with saturation photon number P_{s}, $\Gamma = V/V_{\mathrm{p}}$ is the mode confinement coefficient, V is the volume of laser cavity, V_{p} is the mode volume of laser, $N_{\mathrm{s}} = n_{\mathrm{s}}V$ is the parameter of logarithmic gain with its density n_{s}, $N_{\mathrm{t0}} = n_{\mathrm{t0}}V$ is the carrier number at transparency with its density n_{t0}. $\gamma_{\mathrm{p}} = v_{\mathrm{g}}(\alpha_{\mathrm{m}} + \alpha_{\mathrm{int}})$ is the total photon loss with the group velocity v_{g}, α_{m} is the cavity loss, α_{int} is the internal loss. $\Delta\omega_{\mathrm{m}} = \omega_{\mathrm{m}} - \omega_{\mathrm{th}}$ can be regarded as frequency detuning between external injection light and output light. $\tau_{\mathrm{L}} = 2n_{\mathrm{g}}L/c$ is the round-trip time in the cavity with its length L, c is the light velocity in vacuum, $n_{\mathrm{g}} = c/v_{\mathrm{g}}$ is the group refractive index. η_{i} is the internal quantum efficiency. I is the driving current. q is the unit charge. β_{c} is the optical linewidth enhancement factor. γ_{BQ} is the loss of carriers from the SCH region to the quantum wells and γ_{QB} is the loss of carriers escaping from the active region to the SCH layer. $\gamma_{\mathrm{e}} = A_{\mathrm{nr}} + B(N/V) + C(N/V)^2$ is the total carrier loss in the active layer, A_{nr} is the nonradiative recombination rate, B is the radiative recombination coefficient, C is the Auger recombination coefficient. k is the optical injection factor.

Actually, the all-optical chaotic repeaters can be considered to be a series of synchronous systems controlled by feedback paths. Under suitable parameters, when $t \to \infty$, absolute value $|E_{\mathrm{t}} - E_{\mathrm{r}i}| \to 0$, $|\phi_{\mathrm{t}} - \phi_{\mathrm{r}i}| \to 0$, $|N_{\mathrm{t}} - N_{\mathrm{r}i}| \to 0$, $|N_{\mathrm{Bt}} - N_{\mathrm{Br}i}| \to 0$ $(i = 1, 2, \cdots, n+1)$, therefore, synchronization is realized among the receiver, repeaters, and transmitter.

One of the essential conditions for realizing chaotic secure communication is that the receiver should have the same parameters as the transmitter. We suppose that the transmitter, the repeater, and the receiver have identical parameters here. Defining synchronous error as

$$\Delta_{\mathrm{t},i} = <|E_{\mathrm{t}}(t) - E_{\mathrm{r}i}(t)|>, \quad (3)$$

$$\Delta_{j,i} = <|E_{\mathrm{r}j}(t) - E_{\mathrm{r}i}(t)|>, \quad (4)$$

where the bracket represents average value, $i = 1, 2, \cdots, n+1$, $j = 1, 2, \cdots, n+1$, and $j \neq i$. The parameters in numerical analysis are listed in Table 1. As an example, we illustrate the numerical analysis results with only one repeater system first. When parameters are $\phi_{\mathrm{m}} = 0$, $f = 0$, $k = 0.18$, and $E_{\mathrm{m}} = 0.2529E_{\mathrm{s}}$, chaotic laser attractors are obtained by numerically integrating Eqs. (1) and (2) with different initial values in Fig. 2. The phase spaces in Fig. 2 are constructed by $(N_{\mathrm{t}}, E_{\mathrm{t}})$, $(N_{\mathrm{r1}}, E_{\mathrm{r1}})$, and $(N_{\mathrm{r2}}, E_{\mathrm{r2}})$, respectively. The chaotic attractors of transmitter, repeater, and receiver are shown in Figs. 2(a), (b), and (c), respectively. Their traces are utterly different for different initial values. When $f = 0.504$, we can find in Fig. 3 that the synchronizations are achieved successively each other. The numerical calculation also demonstrates that the synchronization is an asymptotical process. The synchronous errors can reach zero after 8.1, 13.2, and 13.3 ns, respectively. In another word, the whole system is perfectly synchronized after 13.3 ns.

Table 1. Laser Parameters[8]

Symbol	L	V	Γ	n_{g}
Value	1200	50.4	0.045	3.6
Unit	μm	μm^3		
Symbol	n_{s}	α_{m}	α_{int}	n_0
Value	0.1×10^{18}	11.5	20	2.1×10^{18}
Unit		cm^{-1}	cm^{-1}	cm^{-3}
Symbol	A_{nr}	B	C	P_{s}
Value	2.5×10^{8}	1.0×10^{-10}	5.0×10^{-29}	2.2×10^{7}
Unit	s^{-1}	cm^3/s	cm^6/s	
Symbol	g_0	β_{c}	$\Delta\omega$	I
Value	2700	3	$2\pi\times10^{9}$	50
Unit	cm^{-1}		rad/s	mA
Symbol	η_{i}	γ_{BQ}	γ_{QB}	
Value	0.8	2.5×10^{10}	5×10^{9}	
Unit		s^{-1}	s^{-1}	

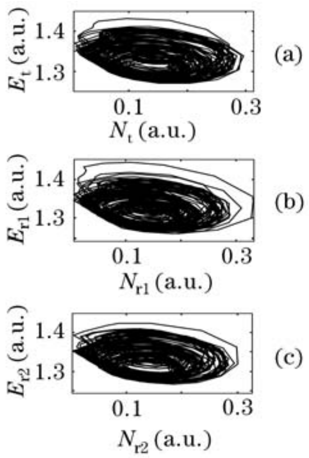

Fig. 2. Chaotic laser attractors of (a) transmitter, (b) repeater, and (c) receiver.

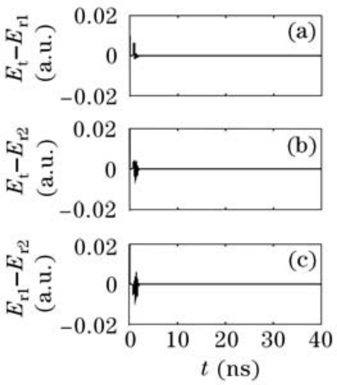

Fig. 3. Synchronizations between (a) transmitter and repeater, (b) receiver and repeater, and (c) transmitter and receiver.

Suppose that a modulation signal $S(t)$ is hidden in chaotic wave. They are transmitted synchronously and received by the repeater "r1". After realizing synchronization between the transmitter and the repeater "r1", the synchronous waves is transmitted by the repeater "r1", then the transmitted signals are received by the receiver "r2". In numerical analysis, the modulation signal $S(t)$ is a sinusoidal function with amplitude $A = 1\%E_0$ ($E_0 = 0.13E_s$) and modulation frequency of 200 MHz. The calculation result is shown in Fig. 4 where $f = 0.72$. The left part is the chaotic decoding, Figs. 4(a), (b), and (c) illustrate the synchronous decoding signals between the repeater and the transmitter, the receiver and the transmitter, the receiver and the repeater, respectively. Obviously, disordered waves are added on the decoded signals because of synchronous errors rising from the signals where synchronous errors are $\Delta_{t,1} = 4.7 \times 10^{-4}$, $\Delta_{t,2} = 1.3 \times 10^{-3}$, and $\Delta_{1,2} = 8.1 \times 10^{-4}$, respectively. The ratio of the signal to the error $A/\Delta_{1,2}$ is about 1.6. The right parts of Fig. 4 illustrate the final decoded signals after filtering, which correspond to the left parts. The dotted lines are the original signals and solid lines are the decoded signals after filtering. We can find that the decoding is well realized by the repeater.

Digital signal with a square wave signal of amplitude $A = 0.5\%E_0$ and 400-Mb/s bit rate is shown in Fig. 5, where $f = 0.792$. Synchronous errors generated by the signal are $\Delta_{t,1} = 3.7 \times 10^{-4}$, $\Delta_{t,2} = 9.2 \times 10^{-3}$, and $\Delta_{1,2} = 5.8 \times 10^{-4}$, respectively, where the ratio $A/\Delta_{1,2} = 1.1$. Similarly, we can find that the digital signal decoding is also well realized by the repeater.

Generally, in order to satisfy different bit rates communications, the repeaters should have a larger modulation bandwidth. The simulation results of encoding and decoding, which just did as the above mentioned, with a digital signal of 20-Gb/s bit rate and amplitude $A = 0.5\%E_0$, is shown in Fig. 6. The synchronous errors produced by the signal are $\Delta_{t,1} = 3 \times 10^{-4}$,

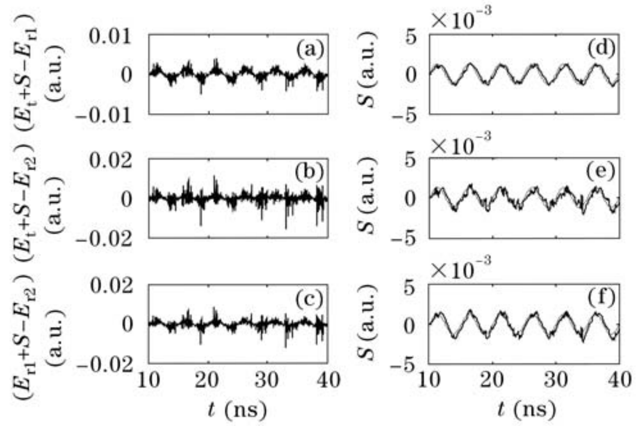

Fig. 4. Analog chaotic communication. The right illustrates filtering and dotted lines indicate the original signals.

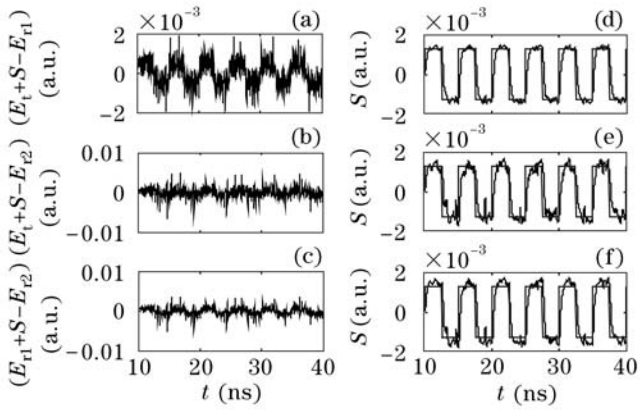

Fig. 5. Digital chaotic communication. The right illustrates filtering and square waves indicate the original signals.

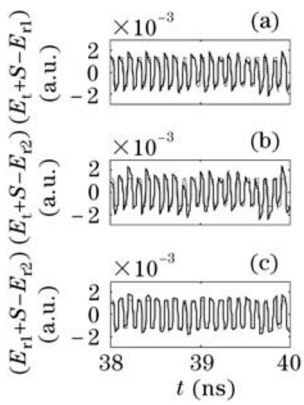

Fig. 6. High bit rate digital chaotic decoding where dotted lines indicate the original signals.

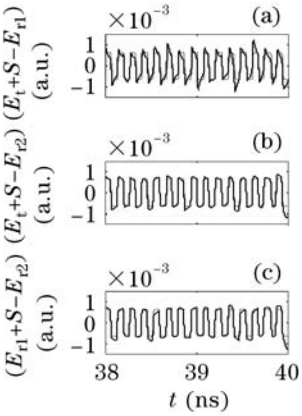

Fig. 7. High bit rate digital chaotic decoding with two repeaters where dotted lines indicate the original signals.

$\Delta_{t,2} = 5.4 \times 10^{-4}$, and $\Delta_{1,2} = 1.9 \times 10^{-4}$, respectively, where the ratio $A/\Delta_{1,2} = 3.4$. The decoded signals still are fine even though without filtering in Fig. 6. We can see that the repeater has really improved decoding quality, especially in high bit rates chaotic communications. A chaotic communication system with two repeaters is also simulated without filtering and its numerical result is illustrated in Fig. 7 with a digital signal of 15-Gb/s bit rate and amplitude $A = 0.5\%E_0$. The synchronous errors are $\Delta_{t,1} = 1.8 \times 10^{-4}$, $\Delta_{1,2} = 1.5 \times 10^{-4}$, $\Delta_{2,3} = 2.3 \times 10^{-4}$, and $\Delta_{t,3} = 4.7 \times 10^{-4}$, respectively, with the ratio $A/\Delta_{2,3} = 2.8$. Therefore, we can deduce that multiple repeaters can also regenerate the original chaotic signal and are suitable for chaotic communication.

In conclusion, we have presented the all-optical chaotic MQW laser repeater for long-haul chaotic secure communication systems, and simulated numerically to show that the synchronizations are well realized among the transmitter, the repeaters, and the receiver. Of course, the system parameters mismatching needs to be further studied. But this repeater system can be used in long-haul optical chaotic secure communications.

This work was supported by the Education Department of Jiangsu Province (No. 04KJD520084 and 02KJD510019). S. Yan's e-mail address is yansenlinbsh@sina.com or senlinyan@163.com.

References

1. J. Z. Xia, H. W. Cai, H. Ren, L. Li, L. Zhao, G. T. Chen, and Z. J. Fang, Acta Opt. Sin. (in Chinese) **23,** 823 (2003).
2. Z. W. Tan, Y. Liu, Y. J. Fu, T. G. Ning, L. Pei, and S. S. Jian, Chin. J. Lasers (in Chinese) **30,** 311 (2003).
3. L. Lü and C. R. Li, Chin. J. Lasers (in Chinese) **30,** 322 (2003).
4. S. Tang and J. M. Liu, IEEE J. Quantum Electron. **39,** 1468 (2003).
5. H. F. Chen and J. M. Lin, IEEE J. Quantum Electron. **36,** 27 (2000).
6. J. Ohtsubo, IEEE J. Quantum Electron. **38,** 1141 (2002).
7. Y. Liu, P. Davis, Y. Takiguchi, T. Aida, S. Saito, and J.-M. Liu, IEEE J. Quantum Electron. **39,** 269 (2003).
8. J. Troger, L. Thévenaz, P.-A. Nicati, and P. A. Robert, J. Lightwave Technol. **17,** 629 (1999).